Biocompatible Luminescent Silicon Quantum Dots for Imaging of Cancer Cells

Folarin Erogbogbo,[†] Ken-Tye Yong,[‡] Indrajit Roy,[‡] GaiXia Xu,[‡] Paras N. Prasad,[‡] and Mark T. Swihart[†,‡,*]

[†]Department of Chemical and Biological Engineering and [‡]Institute for Lasers, Photonics, and Biophotonics, University at Buffalo (SUNY), Buffalo, New York 14260-4200

ABSTRACT Luminescent silicon quantum dots (Si QDs) have great potential for use in biological imaging and diagnostic applications. To exploit this potential, they must remain luminescent and stably dispersed in water and biological fluids over a wide range of pH and salt concentration. There have been many challenges in creating such stable water-dispersible Si QDs, including instability of photoluminescence due their fast oxidation in aqueous environments and the difficulty of attaching hydrophilic molecules to Si QD surfaces. In this paper, we report the preparation of highly stable aqueous suspensions of Si QDs using phospholipid micelles, in which the optical properties of Si nanocrystals are retained. These luminescent micelle-encapsulated Si QDs were used as luminescent labels for pancreatic cancer cells. This paves the way for silicon quantum dots to be a valuable optical probe in biomedical diagnostics.

KEYWORDS: silicon · quantum dot · nanocrystal · micelle encapsulation · *in vitro* imaging

Quantum dots (QDs) have attracted great attention because of their unique optical properties.[1,2] They have been intensively studied for biomedical applications ranging from contrast agents to biological labeling.[3–6] However, a major concern that may limit their use in biology and medicine is the toxicity associated with the cadmium-containing QDs that have been most studied for use in biomedical diagnostics.[7] Although silicon QDs are expected to be far less toxic than group II–VI QDs, they have thus far not been widely used in these systems because of the challenges inherent to making them water-dispersible and compatible with biological fluids. Fabricating colloidally and optically stable water-dispersible Si QDs remains an important challenge in making them useful for *in vitro* and *in vivo* studies. To date, very few studies have reported the production of water-dispersible Si QDs.[8–14] Previously, water dispersible Si QDs have been produced by modifying the nanocrystal surface with carboxylic acids[8,10] or amines.[13] Silicon QDs are more often made dispersible in nonpolar organic solvents because hydrophobic moieties (*e.g.*, styrene and octene) can be more easily attached to the silicon surface.[15–22] However, Si QDs generally show unstable photoluminescence and poor colloidal stability in aqueous environments. PL degradation typically occurs within a few days after preparation of an aqueous dispersion of Si QDs using current methods. Thus, new approaches to making water-dispersible Si QDs while maintaining spectral and colloidal stability continue to be of great interest. Recently, Tilley *et al.* have reported the synthesis of water-dispersible Si QDs with blue luminescence upon anchoring allylamine onto silicon QD surfaces.[11,13] Ruckenstein and coworkers reported the use of red-emitting Si QDs grafted with poly(acrylic acid) for fixed-cell labeling.[8] Our group has recently reported that water dispersible Si QDs with blue, green, and yellow photoluminescence can be obtained by functionalizing them with acrylic acid in the presence of HF.[10] However, these particles have thus far not maintained satisfactory colloidal and spectral stability in biological environments.

Polyethyleneglycol (PEG) grafted (PEGylated) phospholipids self-assemble into micelles with diameters typically smaller than 100 nm in aqueous media. Such phospholipid micelles (also known as diacyllipid micelles or polymeric micelles) are more stable than micelles obtained from conventional detergents (*e.g.*, SDS and CTAB) and have very low critical micelle concentration (CMC) values ($\sim 10^{-6}$ M). In addition to their low CMC, phospholipid micelles have high kinetic stability because of the presence of multiple sites capable of hydrophobic interaction within each polymer molecule. Similar to detergent micelles, polymeric micelles solubilize "oil-like" particles by incorporating them into their

*Address correspondence to swihart@eng.buffalo.edu.

Received for review October 24, 2007 and accepted April 19, 2008.

Published online May 2, 2008.
10.1021/nn700319z CCC: $40.75

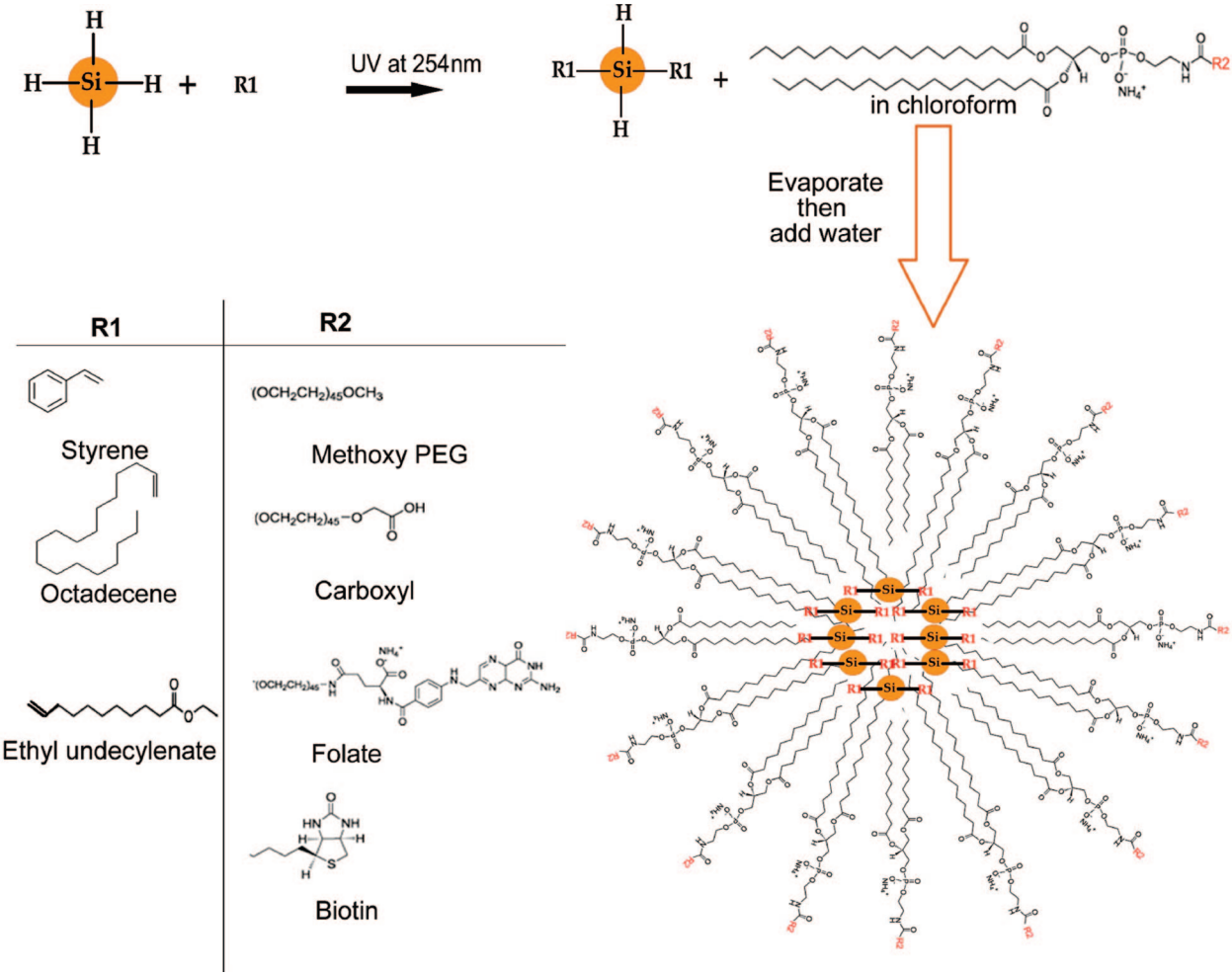

Figure 1. Schematic of surface functionalization of silicon quantum dots followed by micellar encapsulation and a table indicating the compounds (R1) grafted onto the silicon nanoparticles and the functional groups (R2) commercially available on the phospholipids.

hydrophobic core. More importantly, the outer surface of phospholipid micelles displays a dense layer of PEG that is nonimmunogenic and nonantigenic. This favors extended systemic circulation time, broad biodistribution, and lowered toxicity of the encapsulated nanoparticles. Furthermore, the PEG lipids can be functionalized with specific reactive groups for targeting purposes. Though micellar encapsulation of cadmium-based QDs has been demonstrated, we are not aware of any previous reports of producing water-dispersible Si QDs using phospholipid micelles. The most closely related study is on the photoluminescence quenching of silicon nanoparticles within phospholipid vesicle bilayers.[23] Previously, Dubertret *et al*. have reported encapsulation of individual core−shell CdSe/ZnS QDs in phospholipid micelles for *in vitro* and *in vivo* imaging.[24] More importantly, they have discovered that these encapsulated QDs were biocompatible, and displayed low toxicity *in vivo*.

In this work, we report the preparation of water-dispersible and biocompatible Si QDs using phospholipid micelles. The Si QDs were prepared by laser-driven pyrolysis of silane, followed by HF-HNO_3 etching. Styrene, octadecene, or ethyl undecylenate was used to functionalize the Si QD surfaces, thereby rendering them dispersible in chloroform. Phospholipid micelles were then used to enable stable dispersion of Si QDs in water, generating a hydrophilic shell with PEG groups on its surface. These micelle-encapsulated Si QDs were systematically characterized by TEM, HRTEM, EDS, UV−vis, and fluorescence spectrometry. For *in vitro* cell-labeling studies, amine-functionalized phospholipid-PEGs were used to encapsulate Si QDs and these encapsulated particles were used as biological luminescent probes. The uptake of micelle-encapsulated Si QDs into pancreatic cancer cells was confirmed by confocal imaging.

RESULTS AND DISCUSSION

Figure 1 illustrates the functionalization of Si QDs using photoinitiated hydrosilylation followed by encapsulation in phospholipid micelles. Organic molecules with a terminal double bond react with the hydrogen-terminated silicon surface *via* hydrosilylation to give a covalent Si−C linkage on the surface of the Si QD. These QDs are generally dispersible in chloroform, hexane,

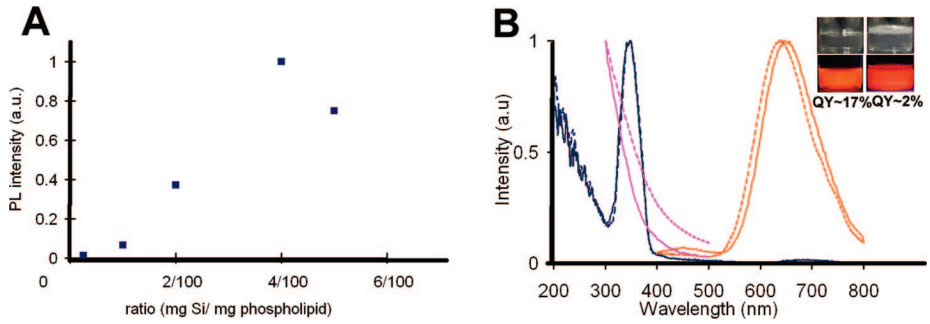

Figure 2. Characterization of micelle-encapsulated Si QDs: (A) PL intensity *vs* Si/phospholipid mass ratio. (B) Optical spectra of Si-QDs in chloroform and micelle-encapsulated QDs in water: PL (orange) absorbance (pink), PLE (blue). Solid lines are ethyl-undecylenate-grafted particles; dotted lines are micelle-encapsulated Si QDs. The inset photos are vials of styrene-grafted (left) and micelle-encapsulated (right) Si QDs under ambient lighting (top) and UV illumination (bottom).

toluene, and other nonpolar solvents. Phospholipid micelles were prepared from PEG-2000-DSPE (from Avanti Polar Lipids). Octadecene, ethyl undecylenate, and styrene functionalized Si QDs were found to be effectively encapsulated in phospholipid micelles.

Figure 2A shows the relationship between the weight ratio of Si QDs to phospholipid and the corresponding photoluminescence intensity. Various volumes of known concentration of Si QD stock solution were mixed with a fixed amount of phospholipids in chloroform solution. We found that the most stable and highest photoluminescence intensity was obtained at the weight ratio of about 4:100, which is probably the optimal ratio for solubilizing most of the hydrophobic Si QDs in the micelle core. Figure 2B shows absorption, PL emission, and PL excitation spectra of the ethyl undecylenate grafted silicon QDs, before and after encapsulation in phospholipids micelles. The micelle-encapsulated Si QD dispersions have optical properties that are nearly identical to those of the Si nanoparticles in chloroform. The difference in the absorption spectra is mainly due to weak absorption by the phospholipids, but scattering from the micelles may also contribute. The inset in Figure 2B shows photoluminescence from the Si QDs in chloroform (left) and micelle encapsulated Si QDs in water (right) under UV (365 nm) illumination from a hand-held lamp. The colloidal stability of the micelle-encapsulated Si particles in water (seen in the top images, under ambient illumination) was attributed to the hydrophilic (PEG) part of the phospholipid surfactant (R2 in Figure 1). The quantum yield (QY) of the styrene-coated Si QDs was estimated to be 17% and the QY for the micelle-encapsulated styrene grafted QDs was estimated to be 2%. The ethyl undecylenate grafted particles encapsulated in micelles had QY above 4%. Although the QY of Si QD in micelles is lower than that of the Si QDs dispersed in an organic solvent, a 1 to 5% QY has been reported to be sufficient for cell-labeling studies.[25] The micelle-encapsulated Si QD solution did not show any significant change in the photoluminescence intensity or exhibit any precipitation even after 2 months of storage at 4 °C.

Figure 3A and B show TEM images of the ethyl-undecylenate-grafted Si QDs. Crystalline Si QDs of about 4 nm are observed. These particles were then encapsulated in micelles, and the micelles were fixed in 4% formaldehyde for 10 min before they were placed on the TEM grid. The TEM images (Figure 3C) show a

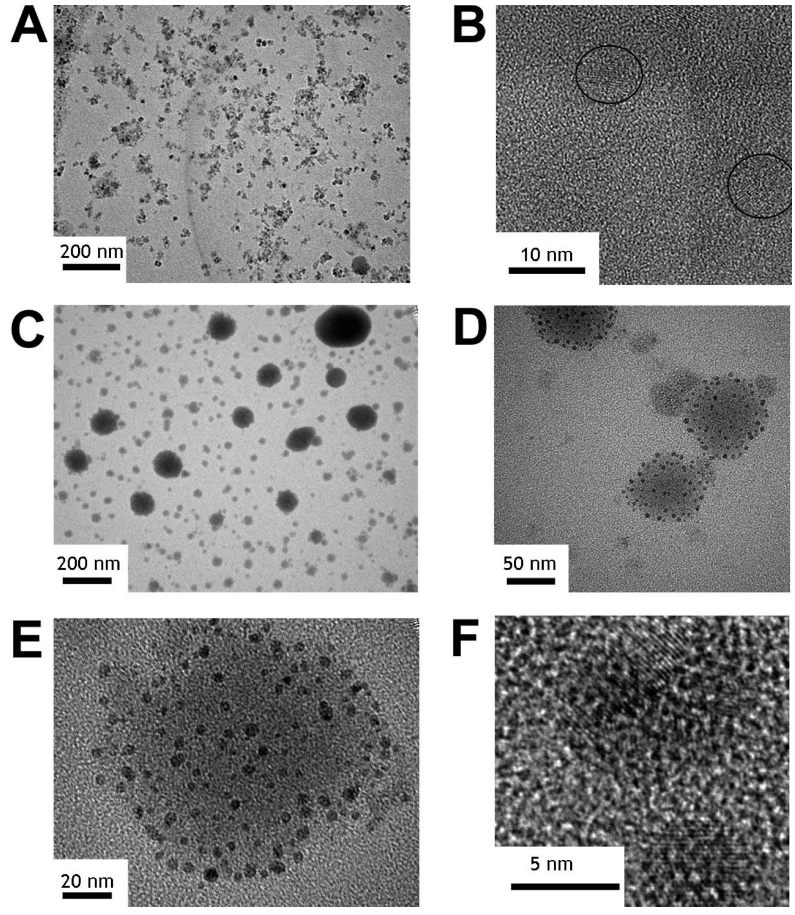

Figure 3. TEM images of (A and B) ethyl-undecylenate-grafted Si QDs cast from a chloroform dispersion; (C and D) micelle-encapsulated Si QDs, fixed with 4% formaldehyde and cast from water; (E) all of the silicon QDs contained in a single micelle; and (F) silicon QDs visible within the micelle

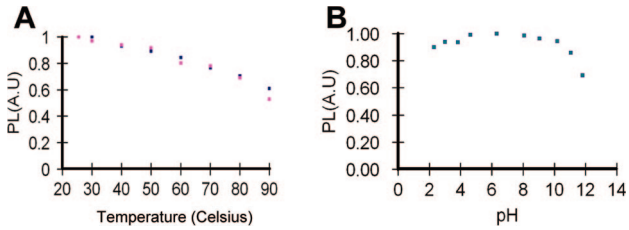

Figure 4. Photoluminescence intensity from micelle encapsulated Si-QDs *vs* (A) temperature and (B) pH.

wide range of sizes for clusters of silicon QD material. A careful examination of Figure 3D indicates the micelle sizes range from 50 to 120 nm. The larger clumps seen in Figure 3C are interpreted as micelle aggregates. Figure 3F shows the lattice fringes of individual crystalline Si QDs within the micelle. Larger versions of Figure 3B and F are available in Supporting Information.

The stability and optical properties of micelle-encapsulated Si QDs under various biologically relevant conditions of pH and temperature were further examined. Figure 4a shows the variation of PL intensity of the water dispersion of Si QDs after heating. Although there is clear temperature dependence, the particles retain more than 50% of their initial PL intensity even after being heated to 90 °C. Over the temperature range of most relevance to biological experiments, 25 to 40 °C, the PL intensity varies by less than 10%. Figure 4b shows the variation of PL intensity of Si QDs in acidic-to-basic pH environments. When the micelle-encapsulated Si QDs are dispersed in HPLC water, the pH of the resulting solution is about 7. From pH 4 to 10, the PL intensity varies by less than 10%, and also remains stable with time (over a month). At pH 12, the PL intensity decreases by about 30%, relative to neutral pH. However, it is worth noting that for the micelle-encapsulated Si QD solution at pH 12, the PL intensity was still maintained for over 2 weeks. On the other hand, at pH 2, a ~10% loss of their PL was observed immediately, and further degradation of the PL was observed after a day of storage at room temperature. The particles also exhibit stable PL when dispersed in common buffers like PBS (pH ≈ 7.2) and MES (pH ≈ 4.6). Compared to HPLC water, the PL intensity of Si QDs in PBS decreased by 5%, and in MES decreased by 3%.

For *in vitro* cell-labeling studies with Si QDs, we used human pancreatic cancer cells (Panc-1) maintained in DMEM medium, with 10% fetal bovine serum (FBS) and appropriate antibiotic. On the day prior to treatment, cells were seeded in 35 mm cell culture dishes. On the day of treatment, the cells, at a confluency of 70−80%, were incubated with the micelle-encapsulated Si QDs at a final concentration of ~8 μg/mL for two hours at 37 °C. After two hours, the cells were washed thrice with PBS and directly imaged using a laser scanning confocal microscope. Figure 5A shows the confocal images of Panc-1 cells stained with amine terminated micelle-encapsulated Si QDs. Figure 5B shows the confocal images of Panc-1 cells stained with transferrin (Tf)-functionalized micelle-encapsulated Si QDs. Tf was conjugated to carboxyl-terminated micelle-encapsulated Si QDs, after micelle formation. Uptake of Si QDs can be clearly observed from the robust optical signal from the cells. Local spectral analysis of the overall cell stain-

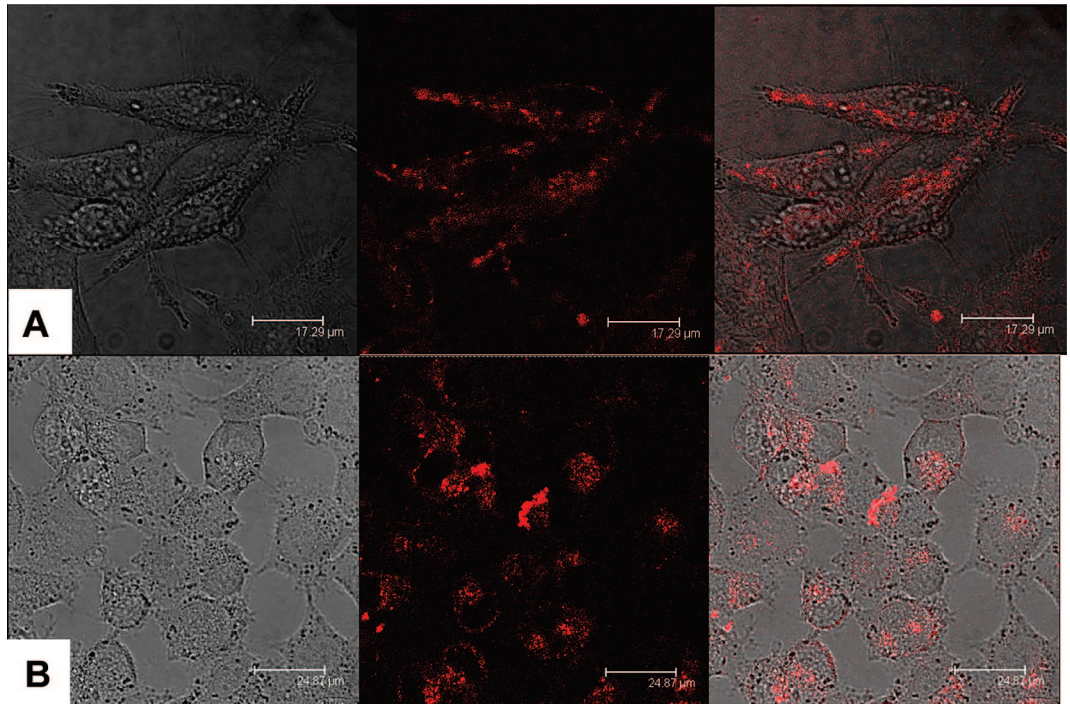

Figure 5. Confocal microscopic visualization of live pancreatic cancer cells treated with (A) amine-terminated micelle encapsulated Si QDs, (B) Tf-conjugated micelle-encapsulated Si QDs. From left to right, the panels show the transmission image, luminescence image, and an overlay of the two. The scale bars are 17.29 and 24.87 μm in A and B, respectively.

ing by the quantum dots (see Supporting Information) confirms that the luminescence signal is from the Si QDs. Control experiments using PEG-terminated micelles, with neither amine nor tranferrin groups on their surface, showed no detectable uptake by the cells (data not shown). This shows that the cellular uptake is sensitive to the functionalization of the micelle surface. These images were obtained using an excitation wavelength of 405 nm, the shortest available on the microscope used. As shown in Figure 2, the peak of the photoluminescence excitation spectrum is near 350 nm, and the PL emission for 405 nm excitation is substantially smaller than the peak. Thus, we expect that much brighter images could be obtained with an excitation source and microscopy system optimized for imaging with the Si QDs. Importantly, we did not observe any signs of morphological damage to the cells upon treatment with the water-dispersible Si QDs. To the best of our knowledge, this is the first report of using Si QDs for imaging live cancer cells. MTS assays were performed to provide a preliminary assessment of the toxicity of the micelle-encapsulated Si QDs. At the concentration used in the imaging shown in Figure 5 (~8 μg/ml), average cell viability was above 95% after 24 h and above 85% at 48 h. Further details are given in Supporting Information.

In conclusion, a procedure for preparing biocompatible Si QDs using PEGylated phospholipids has been described, and their use for imaging of live cancer cells has been demonstrated. This provides a simple, facile, and straightforward method for the production of colloidally and optically stable water-dispersible Si QDs, with no observable *in vitro* toxicity. The dispersion stability and optical properties of the micelle-encapsulated Si QDs were characterized in various biologically relevant conditions. The micelle encapsulated silicon QDs were found to be robustly taken up by pancreatic cancer cells *in vitro*, thereby highlighting their potential to be used as a nontoxic optical probe for biomedical diagnostics.

EXPERIMENTAL METHODS

Photoluminescent Silicon QD Preparation. Silicon nanocrystals were prepared by CO_2 laser pyrolysis of silane in an aerosol reactor based on the method developed by Li *et al.*[20] The resulting powder consisted of nonphotoluminescent crystalline Si particles about 5 to 10 nm in diameter. The etching procedure developed by Hua *et al.*[18] was adopted and modified to reduce the nanocrystal size and break up agglomerated nanocrystals. A 30 mg portion of the Si powder was dispersed in 3 mL of methanol with sonication. An 11 mL aliquot of an acid mixture containing HF (48 wt%) and HNO_3 (69 wt%) (10/1, v/v) was added to the resulting dispersion to initiate etching. As the etching proceeded, the particle size decreased, resulting in visible PL that evolved from red to yellow to green. Upon approaching the desired emission color, etching was slowed by adding about 20 mL of methanol. The particles were collected on a poly(vinylidene fluoride) (PVDF) membrane filter (nominal pore size 100 nm) and washed with a large amount of 1:3 methanol/water mixture to remove any adsorbed acid mixture. The particles were rinsed with pure methanol and then added to the reagent to be used for the photoinitiated hydrosilylation. This process was performed in a glovebox under a nitrogen atmosphere. Sonication was used to disperse the particles, but a stable colloidal dispersion was not formed and the reactor contents appeared cloudy in all cases. The mixtures were transferred into a 40 mL Aldrich Schlenk-type reactor containing a magnetic stirrer. A Rayonet photochemical reactor (Southern New England Ultraviolet Co.) equipped with 16 RPR-2537 Å UV tubes was used to initiate the hydrosilylation reaction. The reaction time required varied substantially depending on the compound being attached to the particles and the particle size.[18] After reaction, a clearer dispersion was obtained. It was drawn through a PTFE syringe filter (pore size 0.45 μm).

Micelle Encapsulation. In a typical experiment, 5 mg of the phospholipid was dispersed in 0.5 mL chloroform in a 10 mL round-bottom flask. An 80 μL portion of silicon quantum dot dispersion (containing ~0.16 mg silicon) was added. Each mixture was gently stirred for 5 to 40 min. A Labconco rotory evaporator with a water bath of 37 °C was used to evaporate the solvents. The lipidic film, deposited on the reaction vial, was hydrated with 3−5 mL of HPLC water and subjected to ultrasonication for 10 min using a bath sonicator. The resulting dispersion was filtered through a 0.2 μm membrane filter and kept at 4 °C for further use.

Photoluminescence and PLE Spectra. Photoluminescence (PL) spectra were recorded using a Perkin-Elmer Luminescence spectrometer (model LS50) with a 390 nm emission cutoff filter. The excitation wavelength was set at 350 nm and the emission scanned from 400 to 800 nm. Photoluminescence excitation (PLE) spectra were recorded using the same spectrometer. The emission wavelength was set at the wavelength of peak emission intensity and the excitation was scanned from 400 to 800 nm. Solution samples of grafted silicon particles were filtered through a syringe filter (PTFE, pore size 450 nm), diluted to a concentration of about 0.01 g/L, and then loaded into a quartz cuvette for measurements.

Quantum Yield Estimates. Fluorescence quantum yields (QYs) of the silicon quantum dot dispersions were determined by comparing the integrated emission from the nanocrystals to rhodamine 6G dye solutions of matched absorbance. Samples were diluted so that they were optically thin. The emission spectra for quantum yield measurements were collected using a Fluorolog-3 Spectrofluorometer (Jobin Yvon; fluorescence spectra).

Temperature Study. Micelle-encapsulated Si QDs were dispersed in water and heated. Samples of the QD solution were extracted at temperatures ranging from ambient to 100 °C, and the fluorescence was measured using a spectrofluorometer.

pH Study. The pH of the micelle-encapsulated Si dispersions was varied by the dropwise addition of NaOH or HCl. The pH was monitored with a Mettler Toledo seven multi-pH meter.

Conjugation of Micelle Encapsulated QDs with Transferrin. A 1 mL portion of micelle-encapsulated Si QD stock solution was mixed with 200 μL of 0.5 mg/mL EDC solution and gently stirred for 2 to 3 min. Next, 200 μL of 2 mg/mL transferrin solution was added into this mixture and stirred at room temperature for 2 h to allow the protein to covalently bind to the micelle-encapsulated Si QDs.

Cellular Imaging. Confocal microscopy images were obtained using a Leica TCS SP2 AOBS spectral confocal microscope (Leica Microsystems Semiconductor GmbH, Wetzler, Germany) with laser excitation at 405 nm. All images were taken with the exact same conditions of laser power, aperture, gain, offset, and scanning speed.

Electron Microscopy. TEM images were obtained using a JEOL 2010 field emission TEM/STEM at the Canadian Center for Electron Microscopy at McMaster University. Samples were drop-cast from dispersions onto a carbon-coated TEM grid and the solvent was evaporated under gentle heating by a lamp. Local energy dispersive X-ray spectra (EDX) were obtained using a Hita-

chi HD-2000 STEM with an Oxford Instruments Inca EDX system at the University of Toronto Centre for Nanostructure Imaging.

Cell Viability. For each MTS assay, 24 culture wells (8 sets, each set contains 3 wells) of Panc-1 cell were prepared. Seven sets were treated with different concentration of silicon quantum dots and one set was the control The complete assay was performed thrice, and results were averaged. Various concentrations of micelle-encapsulated silicon quantum dots ranging from 1 to 32 μg/mL, were added to each well and subsequently incubated with the cells for 24 and 48 h at 37 °C under 5% CO_2. As described in the literature,[26] the absorbance of formazan (produced by the cleavage of MTS by dehydrogenases in living cells) is directly proportional to the number of live cells. After the incubation, 150 μL of MTS reagent was then added to each well and well mixed. The absorbance of the mixtures at 490 nm was measured. The cell viability was calculated as the ratio of the absorbance of the sample well to that of the control well and expressed as a percentage.

Acknowledgment. This study was supported by grants from the NSF IGERT, NCI RO1CA119397, the John R. Oishei Foundation, the Chemistry and Life Sciences Division of the Air Force Office of Scientific Research, the University at Buffalo Gerald Sterbutzel Fund, and the University at Buffalo Interdisciplinary Research and Creative Activities Fund. Support from the Center of Excellence in Bioinformatics and Life Sciences at the University at Buffalo is also acknowledged.

Supporting Information Available: Energy-dispersive X-ray spectroscopy (EDS) analysis of a single micelle; local PL emission spectra from within labeled cells; larger versions of HRTEM images shown in Figure 3 panels B and F; detailed results of MTS cell viability assays. This material is available free of charge *via* the Internet at http://pubs.acs.org.

REFERENCES AND NOTES

1. Prasad, P. N. *Nanophotonics*; Wiley-Interscience: New York, 2004.
2. Alivisatos, A. P. Semiconductor Clusters, Nanocrystals, And Quantum Dots. *Science* **1996**, *271*, 933–937.
3. Prasad, P. N. *Introduction to Biophotonics*; Wiley-Interscience: Hoboken, NJ, 2003.
4. Gao, X.; Yang, L.; Petros, J. A.; Marshall, F. F.; Simons, J. W.; Nie, S. *In Vivo* Molecular and Cellular Imaging with Quantum Dots. *Curr. Opin. Biotechnol.* **2005**, *16*, 63–72.
5. Medintz, I. L.; Uyeda, H. T.; Goldman, E. R.; Mattoussi, H. Quantum Dot Bioconjugates for Imaging, Labelling and Sensing. *Nat. Mater.* **2005**, *4*, 435–446.
6. Wolfgang, J. P.; Teresa, P.; Christian, P. Labelling of Cells with Quantum Dots. *Nanotechnology* **2005**, *16*, R9–R25.
7. Derfus, A. M.; Chan, W. C. W.; Bhatia, S. N. Probing the Cytotoxicity of Semiconductor Quantum Dots. *Nano Lett.* **2004**, *4*, 11–18.
8. Li, Z. F.; Ruckenstein, E. Water-Soluble Poly(acrylic acid) Grafted Luminescent Silicon Nanoparticles and Their Use as Fluorescent Biological Staining Labels. *Nano Lett.* **2004**, *4*, 1463–1467.
9. Parak, W. J.; Gerion, D.; Zanchet, D.; Woerz, A. S.; Pellegrino, T.; Micheel, C.; Williams, S. C.; Seitz, M.; Bruehl, R. E.; Bryant, Z.; Bustamante, C.; Bertozzi, C. R.; Alivisatos, A. P. Conjugation of DNA to Silanized Colloidal Semiconductor Nanocrystalline Quantum Dots. *Chem. Mater.* **2002**, *14*, 2113–2119.
10. Sato, S.; Swihart, M. T. Propionic-Acid-Terminated Silicon Nanoparticles: Synthesis and Optical Characterization. *Chem. Mater.* **2006**, *18*, 4083–4088.
11. Tilley, R. D.; Yamamoto, K. The Microemulsion Synthesis of Hydrophobic and Hydrophilic Silicon Nanocrystals. *Adv. Mater.* **2006**, *18*, 2053–2056.
12. Wang, L.; Reipa, V.; Blasic, J. Silicon Nanoparticles as a Luminescent Label to DNA. *Bioconjugate Chem.* **2004**, *15*, 409–412.
13. Warner, J. H.; Hoshino, A.; Yamamoto, K.; Tilley, R. D. Water-Soluble Photoluminescent Silicon Quantum Dots. *Angew. Chem., Int. Ed.* **2005**, *44*, 4550–4554.
14. Zhang, X. M.; Neiner, D.; Wang, S. Z.; Louie, A. Y.; Kauzlarich, S. M. A New Solution Route to Hydrogen-Terminated Silicon Nanoparticles: Synthesis, Functionalization and Water Stability. *Nanotechnology* **2007**, *18*, 095601.
15. Baldwin, R. K.; Pettigrew, K. A.; Garno, J. C.; Power, P. P.; Liu, G. y.; Kauzlarich, S. M. Room Temperature Solution Synthesis of Alkyl-Capped Tetrahedral Shaped Silicon Nanocrystals. *J. Am. Chem. Soc.* **2002**, *124*, 1150–1151.
16. English, D. S.; Pell, L. E.; Yu, Z.; Barbara, P. F.; Korgel, B. A. Size Tunable Visible Luminescence from Individual Organic Monolayer Stabilized Silicon Nanocrystal Quantum Dots. *Nano Lett.* **2002**, *2*, 681–685.
17. Hua, F.; Erogbogbo, F.; Swihart, M. T.; Ruckenstein, E. Organically Capped Silicon Nanoparticles with Blue Photoluminescence Prepared by Hydrosilylation Followed by Oxidation. *Langmuir* **2006**, *22*, 4363–4370.
18. Hua, F.; Swihart, M. T.; Ruckenstein, E. Efficient Surface Grafting of Luminescent Silicon Quantum Dots by Photoinitiated Hydrosilylation. *Langmuir* **2005**, *21*, 6054–6062.
19. Li, X.; He, Y.; Swihart, M. T. Surface Functionalization of Silicon Nanoparticles Produced by Laser-Driven Pyrolysis of Silane followed by HF-HNO_3 Etching. *Langmuir* **2004**, *20*, 4720–4727.
20. Li, X.; He, Y.; Talukdar, S. S.; Swihart, M. T. Process for Preparing Macroscopic Quantities of Brightly Photoluminescent Silicon Nanoparticles with Emission Spanning the Visible Spectrum. *Langmuir* **2003**, *19*, 8490–8496.
21. Linford, M. R.; Fenter, P.; Eisenberger, P. M.; Chidsey, C. E. D. Alkyl Monolayers on Silicon Prepared from 1-Alkenes and Hydrogen-Terminated Silicon. *J. Am. Chem. Soc.* **1995**, *117*, 3145–3155.
22. Ruckenstein, E.; Li, Z. F. Surface Modification and Functionalization through the Self-Assembled Monolayer and Graft Polymerization. *Adv. Colloid Interface Sci.* **2005**, *113*, 43–63.
23. Jang, H.; Pell, L. E.; Korgel, B. A.; English, D. S. Photoluminescence Quenching of Silicon Nanoparticles in Phospholipid Vesicle Bilayers. *J. Photochem. Photobiol. A: Chem.* **2003**, *158*, 111–117.
24. Dubertret, B.; Skourides, P.; Norris, D. J.; Noireaux, V.; Brivanlou, A. H.; Libchaber, A. *In Vivo* Imaging of Quantum Dots Encapsulated in Phospholipid Micelles. *Science* **2002**, *298*, 1759–1762.
25. Zimmer, J. P.; Kim, S. W.; Ohnishi, S.; Tanaka, E.; Frangioni, J. V.; Bawendi, M. G. Size Series of Small Indium Arsenide-Zinc Selenide Core-Shell Nanocrystals and Their Application to *In Vivo* Imaging. *J. Am. Chem. Soc.* **2006**, *128*, 2526–2527.
26. Ding, H.; Yong, K. T.; Roy, I.; Pudavar, H. E.; Law, W. C.; Bergey, E. J.; Prasad, P. N. Gold Nanorods Coated with Multilayer Polyelectrolyte as Contrast Agents for Multimodal Imaging. *J. Phys. Chem. C* **2007**, *111*, 12552–12557.